RSC Advances

ROYAL SOCIETY OF CHEMISTRY

www.rsc.org/advances

RSC Advances

ARTICLE

Molecular Basis of R294K Mutation Effects of H7N9 Neuraminidases with Drugs and cyclic peptides: An in Silico and Experimental Study

Received 00th January 20xx,

Accepted 00th January 20xx

DOI: 10.1039/x0xx000000x

www.rsc.org/

Yeng-Tseng Wang[a,b*] , Lea-Yea Chuang[a] and Chi-Yu Lu[a]

In China, the recent outbreak of the new R294K H7N9 influenza has infected 134 people and killed 45 people since January 2014. Prof. Gaoet al. reported that a R294K neuraminidase (Shanghai N9: R294K mutation; Anhui N9: no R294K mutation) results in multi-drug resistance with extreme oseltamivir resistance (over 100 000-fold). Herein, we report the findings of molecular simulations and computational alanine-scanning mutagenesis for the cyclic peptide I with the neuraminidases of the Shanghai N9 and Anhui N9. A. Our results suggest that the cyclic peptide I can inhibit the Shanghai N9 and Anhui N9 influenza A virus neuraminidase. This peptide can provide the efficient binding affinities to Shanghai N9 neither by the five residues (Arg119, Ile277, Lys294, Arg372 and Tyr406) mutations nor by the 13 residues (Val117, Gln137, Thr149, Hie151, Asp152, Ser154, Ile224, Asn296, Asn347, Asn348, Ile429, Pro433 and Lys434) analyzed by binding mode analysis. However, the four residues (Ile150, Arg153, Gln155 and Arg157) can obviously affect the binding interactions among the cyclic peptide.

1. Introduction

Influenza A virus contains two major surface glycoproteins, neuraminidase (NA) and hemagglutinin (HA). The balance of HA and NA activities has been considered to be critical for influenza virus infectivity and transmissibility.(reference?) H7N9 is a strain of influenza A virus and normally circulates amongst avian populations with some variants known to occasionally infect humans. In China, the recent outbreak of the new R294K H7N9 has infected 134 people and killed 45 people since January 2014. Prof. Gao et al. reported that a R294K neuraminidase (Shanghai N9: R294K mutation; Anhui N9: no R294K mutation) results in multi-drug resistance with extreme oseltamivir resistance (over 100 000-fold).1 The transfer function (ΔGbind = -RT ln(IC50)) is used to transfer the IC50 values to the experimental binding free energies (ΔGbind) values. For oseltamivir (G39), the ΔGbind of wild type of neuraminidase (Anhui N9) is equal to -12.91 kcal/mol (IC50= 0.79 nM), and the ΔGbind of R294K mutation neuraminidase (Shanghai N9) is equal to -5.20 kcal/mol (IC50= 214770 nM). For zanamivir (ZMR), the ΔGbind of wild type of neuraminidase (Anhui N9) is equal to -13.31 kcal/mol (IC50= 0.41 nM), and the ΔGbind of R294K mutation neuraminidase (Shanghai N9) is equal to -10.10 kcal/mol (IC50= 75.7 nM). For peramivir (BCZ), the ΔGbind of wild type of neuraminidase (Anhui N9) is equal to -13.33 kcal/mol (IC50= 0.40 nM), and the ΔGbind of R294K mutation neuraminidase (Shanghai N9) is equal to -12.91 kcal/mol (IC50= 0.79 nM). The calculated binding affinities (ΔGbind) of BCZ, G39 and ZMR inhibitors are very close to the experimental data (Table 3-4 and the calculation of binding affinities (ΔGbind) of BCZ, G39 and ZMR inhibitors are listed in supporting information).Therefore, we used the experimental data of BCZ, G39 and ZMR inhibitors to compare with the N9/cyclic peptides complex systems. Although the zanamivir and peramivir still can inhibit the Shanghai N9, the antiviral activity has been lost in oseltamivir. Thus the new antivirus drugs must therefore be developed.

The neuraminidase is to cleave the terminal linkage of the sialic acid receptor, which results in the release of the progeny virions from the infected host cells. In addition, neuraminidase plays an important role in facilitating the early process of the infection of lung epithelial cells by the influenza virus.2 Because of its essential role in influenza virus replication and its highly conserved active sites, neuraminidase has been an attractive target for the development of novel anti-influenza drugs.3-10 Neuraminidase has been grouped into nine different subtypes (N1-N9) based upon antigenicity.11 Additionally, neuraminidase is further classified into two groups: group 1 (N1, N4, N5 and N8) and group 2 (N2, N3, N6, N7 and N9), based upon primary sequence. This R294K neuraminidase of the 2013 H7N9 influenza A virus (Shanghai N9) has also been reported that five residues (Arg119, Ile277, Lys294, Arg372 and Tyr406) are the key residues for drug-neuraminidase binding.1

Peptides can bind with exquisite specificity to their in vivo targets, resulting in exceptionally high potencies of action and relatively few off-target side effects. This high degree of selectivity in their interactions is the product of millions of years of evolutionary selection for complementary shapes and

[a]*Department of Biochemistry, College of Medicine, Kaohsiung Medical University, Kaohsiung, Taiwan*
[b]*Center for Biomarkers and Biotech Drugs, Kaohsiung Medical University, Kaohsiung, Taiwan*
** Corresponding author: Yeng-Tseng Wang, Ph.D.;100, Shih-Chuan 1st Road, Kaohsiung, 80708, Taiwan, Republic of China; TEL: 886-07-3121101 ext 2138 ; E-mail: c00jsw00@kmu.edu.tw* † Footnotes relating to the title and/or authors should appear here.
Electronic Supplementary Information (ESI) available: Table S1: Detail information of Free energy of computational alanine-scanning mutagenesis calculations of the cyclic peptide I with Shanghai N9 influenza A virus neuraminidase. See DOI: 10.1039/x0xx00000x

sizes from among a huge array of structural and functional diversity. Peptides can be fine-tuned to interact specifically with biological targets, such as potent endogenous hormones, growth factors, neurotransmitters, immunologic agents and signaling molecules. Although peptides have many valuable applications in medicine, so far peptide synthesis still has been severely limited by high clearance, poor membrane permeability, low systemic stability and high costs of manufacture. Recently, more than 100 peptide drugs have already reached the market, such as oxytocin (8 residues), calcitonin (32 residues, hypercalcemia, osteoporosis), teriparatide (34 residues, parathyroid hormone analog, osteoporosis) and enfuvirtide (36 residues, enfuvirtide, antiretroviral).12-15 Cyclic peptides are polypeptide chains wherein the amino termini and carboxyl termini, amino termini and side chain, carboxyl termini and side chain, or side chain and side chain are linked with a covalent bond that generates the ring. A number of cyclic peptides have been discovered in nature and many cyclic peptides have been synthesized in the laboratory. Cyclic peptides have several applications in medicine and biology. Recently, a cyclic peptide (Table 1; USA patent: US20130261048) has been reported to efficiently inhibit the neuraminidases of Influenza A or B virus. Thus the objective of our research is to discover novel drugs for Shanghai N9 by using cyclic peptides as neuraminidase inhibitors. Alanine-scanning mutagenesis is an useful technique in the determination of the catalytic or functional sites of protein residues.16 Since alanine amino residue does not alter the main-chain conformation nor does it impose extreme electrostatic or steric effects, alanine is the substitution residue of choice. Sometimes bulky amino acids such as phenylalanine or tyrosine are used in cases where conservation of the size of mutated residues is needed. This technique can also be used to determine whether the side chain of a specific residue plays a significant role in bioactivity. Computational alanine-scanning mutagenesis methods developed from bioinformatics and molecular mechanics can predict important residues of protein-small compounds interactions. As a computational method, the computational alanine-scanning mutagenesis method17 can predict the important residues in protein-small compounds interactions.18 Here the SIE (solvated interaction energies)17 alanine-scanning mutagenesis method was performed for validating the drug-resistance issue of the Shanghai N9 R294K H7N9 influenza A virus neuraminidase. In the present study, the Shanghai N9 and Anhui N9 with the cyclic peptide I were studied with molecular dynamics (MD) simulations, binding free energy calculations. The Shanghai N9 with the cyclic peptide was analyzed by computational alanine-scanning mutagenesis calculations. Our simulations are to gain further insight into the binding interactions between Shanghai N9 and the cyclic peptide.

Table 1. Cyclic peptide

Number of cyclic peptide	Amino sequence in one-letter or drug name
I	CGQRETPEGAEAKPWYC

2. Results and discussion

2.1 Binding modes of Shanghai N9 influenza A virus neuraminidase with the cyclic peptide.

In comparison, the cyclic peptide I have different binding modes with the Shanghai N9 influenza A virus neuraminidase and the analysis of our simulations is shown in Table 2-3 and Figure S1. The overall results of our simulations and the X-ray crystal information1, 19 suggest that Arg153, Asn347, Arg119, Arg372, Hie151, Lys294, Asp152, Asn348 and Asn347 can form hydrogen bonds with the R294K H7N9 neuraminidase. The Asn200, Asn348, Ile150, Asp152, Arg119, Lys434, Hie151, Pro433, Ile429, and Ile224 can form the non-bonding interactions with the R294K H7N9 neuraminidase. In comparing with our results (most frequent residues in Table 2-3 and Figure S1) and the recent report1, the 22 residues (Val117, Arg119, Gln137, Thr149, Ile150, Hie151, Asp152, Arg153, Ser154, Gln155, Arg157, Ile224, Ile277, Lys294, Asn296, Asn347, Asn348, Arg372, Tyr406, Ile429, Pro433 and Lys434) are subjected to be key residues for Shanghai N9. This R294K neuraminidase of the 2013 H7N9 influenza A virus (Shanghai N9) has also been reported that five residues (Arg119, Ile277, Lys294, Arg372 and Tyr406) are the binding key residues for drug-neuraminidase binding.1 The Table 2-3 show that the cyclic peptide can interact with these binding key residues for drug-neuraminidase binding.1

Table 2. Analysis of the binding modes of the cyclic peptide I with the shanghai N9 neuraminidase

Number of cyclic peptide	Hydrogen bonding	Non-bonding
I	Gln155, Asn347, Asn348, Arg372, Arg153, Ile150, Arg157, Gln137	Ile224, Asn296, Lys294, Tyr406, Pro433, Hie151, Lys434, Ile429, Arg119, Thr149, Ser154, Val117, Asp152

Table 3. The detail binding information of the cyclic peptide I with the shanghai N9 neuraminidase

Number of residue (cyclic peptide I)	Hydrogen bonding	Non-bonding
Cys1	Null	Ans296, Ile224
Gly2	Null	null
Gln3	Null	null
Arg4	Null	Asp152
Glu5	Gln155*	Ile224
Thr6	Null	Hie151, Asp152
Pro7	Glu137, Arg157	Hie151, Asp152
Glu8	Arg157*, Ile150	Hie151, Pro433, Thr149, Ser154
Gly9	Null	Pro433, Arg119
Ala10	Null	Pro433
Glu11	Arg153	Hie151, Lys294, Asn296
Ala12	Null	Tyr406
Lys13	Null	Asn348
Pro14	Null	Null
Trp15	Asn347	Null
Tyr16	Null	Hie151, Lys294, Asn296
Cys17	Null	Hie151

*two hydrogen bonds

2.2 Binding free energy of Shanghai N9 and Anhui N9 influenza A virus neuraminidase with the cyclic peptide I.

The binding free energy of each drug was obtained from the 900 ns MD simulation and the SIE method, with both processes using the same parameters. All the results are listed in Table 4-5 and Figure 1. For Shanghai N9, the binding free energies of the cyclic peptides I is -8.26 ± 0.29 kcal/mol, respectively. For Anhui N9, the binding free energies of the cyclic peptides I is -8.24 ±0.53 kcal/mol, respectively. In comparison with our simulation and experimental binding free energies of the three drugs (G39, ZMR and BCZ), the cyclic peptide I may provide the efficient binding affinities with Anhui N9 and Shanghai N9 influenza A virus neuraminidase. The SIE calculations are shown in Table 4-5.

Table 4. Binding free energies of the cyclic peptide/BZC/G39/ZMR with Shanghai N9 influenza A virus neuraminidase

Number of cyclic peptide	Inter vdW	Inter Coulomb	Reaction Field	Cavity	Constant	Predicting ΔGBinding (kcal/mol)	Experimental ΔGBinding (kcal/mol)
I	-90.05±1.03	-90.94±1.86	156.34 ± 1.33	-26.68 ± 0.36	-2.89	-8.26 ± 0.33	-8.56*
BCZ	-36.70 ±2.31	-135.21 ± 4.20	90.28 ±3.07	-8.16 ± 0.17	-2.89	-11.35 ± 0.23	-12.911
G39	-21.03 ± 1.41	-97.16 ± 3.81	98.59 ± 3.02	-6.79 ± 0.07	-2.89	-5.65 ± 0.28	-5.201
ZMR	-30.15 ± 1.07	-110.31 ± 3.02	83.54 ± 2.47	-6.53 ± 0.07	-2.89	-9.74 ± 0.16	-10.101

*our experimental result

Table 5. Binding free energies of the cyclic peptide/BZC/G39/ZMR with Anhui N9 influenza A virus neuraminidase

Number of cyclic peptide	Inter vdW	Inter Coulomb	Reaction Field	Cavity	Constant	Predicting ΔGBinding (kcal/mol)	Experimental ΔGBinding (kcal/mol)
I	-85.49 ± 1.17	-86.18 ± 1.57	149.74 ± 1.08	-29.19 ± 0.38	-2.89	-8.24 ± 0.38	-8.75*
BCZ	-33.68 ±1.83	-141.75 ± 3.81	86.56 ± 4.12	-7.87 ± 0.06	-2.89	-13.02 ± 0.37	-13.331
G39	-34.97 ± 2.74	-135.35 ± 4.57	83.82 ± 2.71	-7.76 ± 0.17	-2.89	-12.75 ± 0.31	-12.911
ZMR	-30.23 ± 2.13	-135.81 ± 2.96	81.81 ± 3.18	-7.85 ± 0.07	-2.89	-12.53 ± 0.63	-13.311

*our experimental result

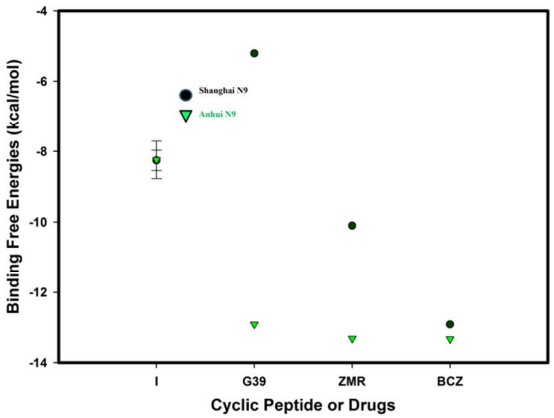

Figure 1. The binding free energies of the cyclic peptide, oseltamivir (G39), peramivir (BCZ), oseltamivir (G39), zanamivir (ZMR) to Shanghai N9 and Anhui N9 influenza A virus neuraminidase .

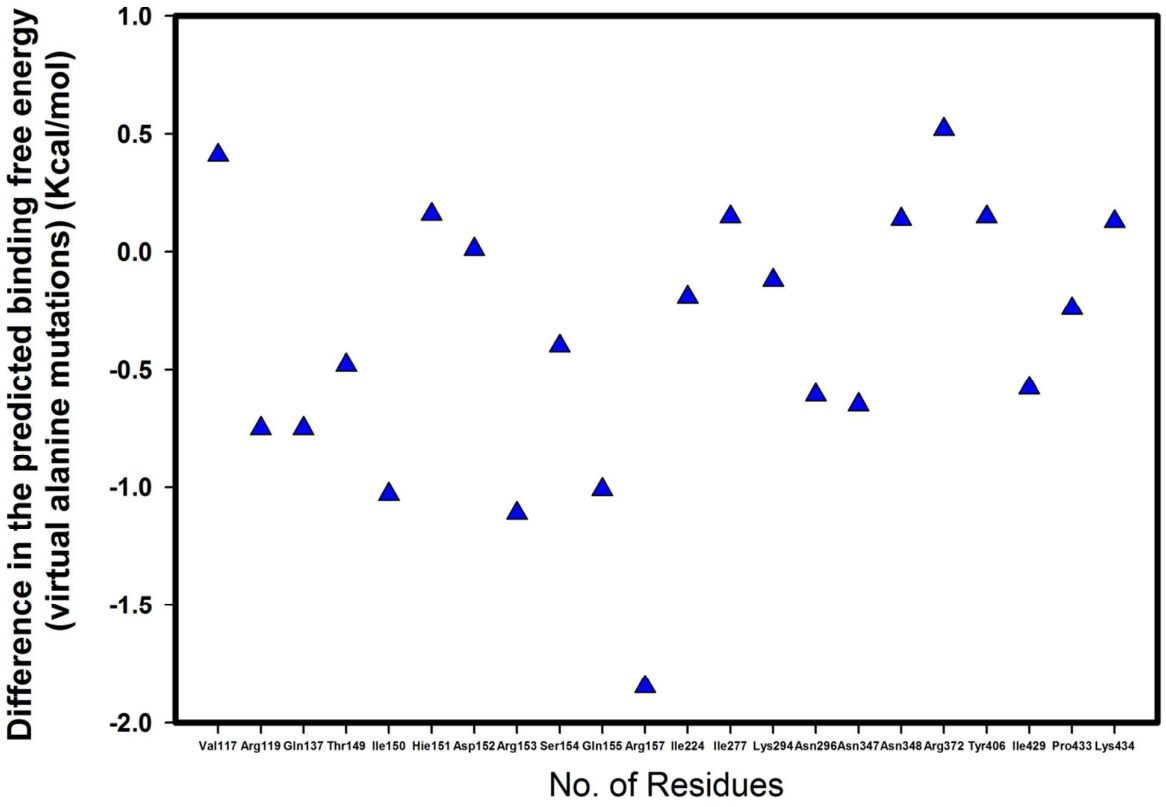

Figure 2. Difference in the predicted binding free energy of the virtual alanine mutations of the cyclic peptide I to Shanghai N9 influenza A virus neuraminidase (Table S1)

RSC Advances

ARTICLE

2.3 Computational alanine-scanning mutagenesis calculations of the binding modes of the cyclic peptide I with Shanghai N9 influenza A virus neuraminidase.

The 22 residues (Val117, Arg119, Gln137, Thr149, Ile150, Hie151, Asp152, Arg153, Ser154, Gln155, Arg157, Ile224, Ile277, Lys294, Asn296, Asn347, Asn348, Arg372, Tyr406, Ile429, Pro433 and Lys434), which are analyzed by binding mode analysis, were mutated to alanine for computational alanine-scanning mutagenesis calculations. The binding free energy of each drug was obtained from the 1000 ns MD simulation and the SIE method, with both processes using the same parameters. All the results are listed in Table S1 and Figure 2. The computational alanine-scanning mutagenesis calculations of the 4 residues (Ile150, Arg153, Gln155 and Arg157) can obviously affect the binding interactions among the cyclic peptide. The ΔGdiff of Ile150, Arg153, Gln155 and Arg157 are -1.03, -1.11, -1.01 and -1.85 kcal/mol, respectively. The mutation of Ile150 caused a net reduction in hydrogen bonding and the inter coulomb/VWD interactions loss (coulomb interaction: -90.94 ± 1.86 to -87.17 ± 2.75; VWD interaction: -90.05 ±1.86 to -82.64 ± 1.48 kcal/mol). The mutation of Arg153 caused a net reduction in hydrogen bonding and the inter coulomb/VWD interactions loss (coulomb interaction: -90.94 ± 1.86 to -79.13 ± 2.71; VWD interaction: -90.05 ±1.86 to -81.65 ± 1.47 kcal/mol). The mutation of Gln155 caused a net reduction in hydrogen bonding and the inter coulomb/VWD interactions loss (coulomb interaction: -90.94 ± 1.86 to -84.14 ± 2.72; VWD interaction: -90.05 ±1.86 to -84.32 ± 1.47 kcal/mol). The mutation of Arg157 caused three net reductions in hydrogen bonding and the inter coulomb/VWD interactions loss (coulomb interaction: -90.94 ± 1.86 to -71.54 ± 2.51; VWD interaction: -90.05 ±1.86 to -87.32 ± 1.11 kcal/mol). In comparison with Table S1 and Figure 2, the differences in the binding free energy (ΔG_{Diff}) of the residue mutations of Ile150, Arg153, Gln155 and Arg157 could affect the binding interactions among the cyclic peptide I.

2.4 Neuraminidase enzyme assay.

For Shanghai N9 and Anhui N9, the IC50 values of the cyclic peptide I are 910 and 670 nM, respectively. The transfer function (ΔGbind = -RT ln(IC50)) is used to transfer the IC50 values to the experimental binding free energies (ΔGbind) values. For Shanghai N9/cyclic peptide I, the ΔGbind is equal to -8.56 kcal/mol. For Anhui N9/cyclic peptide I, the ΔGbind is equal to -8.75 kcal/mol. Although the IC50 values of the cyclic peptide are great than the IC50 values of the ZMR and BCZ drugs, the IC50 values of the cyclic peptide are less than the IC50 values of G39 (Shanghai N9). We suggest the cyclic peptide can be potential drugs for Shanghai N9 and Anhui N9 influenza A virus disease treatment.

3. Materials and Methods

3.1 3D structures design of cyclic peptide I and neuraminidases.

The cyclic peptides structure was generate by Discovery Studio visualizer. Then the cyclic peptide was subjected to optimzie the 3D structures with VEGA ZZ software.[20] Initial cyclic peptides/ neuraminidase (PDB ID: 4MXS for Shanghai N9; PDB ID: 4MWQ for Anhui N9) complex structures were generated by Autodock vina software. Autodock vina is a fast and accurate way to dock drugs into fixed protein binding sites, utilizing NNscore 2.0[21] and several types of genetic algorithms. Four thousand conformations were obtained from docking for the cyclic peptide and then scored by NNscore function. The conformations of the best NNscores were then selected for subsequent MD simulations and solvated interaction energies (binding free energies) calculations. Figure 3 shows the overview of Shanghai N9/cyclic peptide I complex structure.

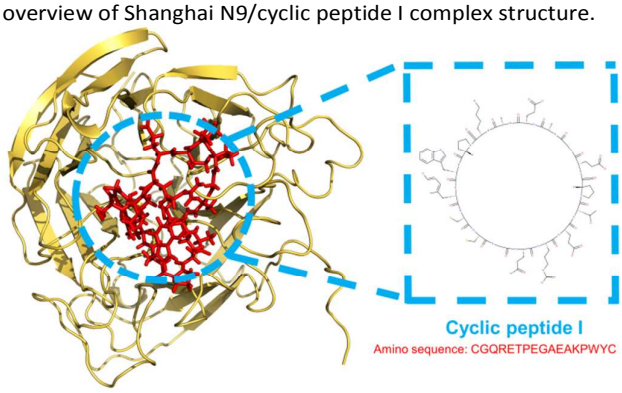

Figure 3. Overview of shanghai N9/cyclic peptide I complex structure. The Shanghai N9 is shown in the cartoon model (colored in orange-yellow) and the cyclic peptide I is shown in the ball-stick model (colored in red).

3.2 Computational models of the cyclic peptide I and neuraminidases.

Our models were then calculated with the AMBER 14 (pmemd.cuda)[21-23] package using the AMBER ff12SB all-hydrogen amino acid parameter.[24] Each complex was solvated in TIP3P[25] water using a truncated hexahedron periodic box extending at least 10 Å from the complex. Nearly 10000 water molecules were added to solvate the complex, with the resulting box size nearly 80.21 × 82.71 × 90.12 Å^3. All MD simulations were performed in the canonical ensemble with a simulation temperature of 310 K, unless stated otherwise, by using the Verlet integrator with an integration time step of 0.002 ps and SHAKE constraints[26] of all covalent bonds involving hydrogen atoms. In the electrostatic interactions, atom-based truncation was performed using the PME[27] method, and the switch van

der Waals function was used with a 2.00 nm cutoff for atom-pair lists. The complex structure was minimized for 100,000 conjugate gradient steps, and was then subjected to a 1000 ns isothermal, constant volume MD simulation. Moreover, the final structures from these simulations were used in the solvated interaction energies (SIE) calculations, and were used to analyze the binding modes of the cyclic peptides with Shanghai N9. The important residues of our results (binding mode analysis from Shanghai N9) and the 22 residues (Val117, Arg119, Gln137, Thr149, Ile150, Hie151, Asp152, Arg153, Ser154, Gln155, Arg157, Ile224, Ile277, Lys294, Asn296, Asn347, Asn348, Arg372, Tyr406, Ile429, Pro433 and Lys434) were subjected to computational alanine-scanning mutagenesis. Figure 4-5 of the complex structures (both Anhui and Shanghai N9/cyclic peptide I/G39/ZMR/BCZ) were equilibrated at 100 ns. Each of the complex structure was sampled 900 ns (99000 snapshots) for binding free energies (SIE) calculations. The snapshots of Shanghai N9/cyclic peptide I were subjected to computational alanine-scanning mutagenesis calculations. Our models with the three drugs were then simulated with the AMBER package using the AMBER FF12SB all-hydrogen amino acid and general amber force field (GAFF) parameters. The geometries of the three compounds were fully optimized and their electrostatic potentials were obtained using single-point calculation, both at the Hatree-Fock level with the 6-31G(d,p) basis set using the GAUSSIAN 09 program. Subsequently, their partial charges were obtained with the restrained electrostatic potential (RESP) procedure using Antechamber. The initial structures are shanghai N9 (PDB ID: 4MWW for G39; 4MWX for ZMR; 4MW0 for BCZ) and Anhui N9 complex structures (PDB ID: 4MWQ for G39; 4MWR for ZMR; 4MWV for BCZ). Then these complex structures were inserted into the TIP3P water box. All MD simulations were performed in the canonical ensemble with a simulation temperature of 310 K, unless stated otherwise, by using the Verlet integrator with an integration time step of 0.002 ps and SHAKE constraints of all covalent bonds involving hydrogen atoms. In the electrostatic interactions, atom-based truncation was performed using the PME method, and the switch van der Waals function was used with a 2.00 nm cutoff for atom-pair lists. The complex structure was minimized for 100,000 conjugate gradient steps, and was then subjected to a 1000 ns isothermal, constant volume MD simulation. The final structures from these simulations were used in the solvated interaction energies (SIE) calculations.

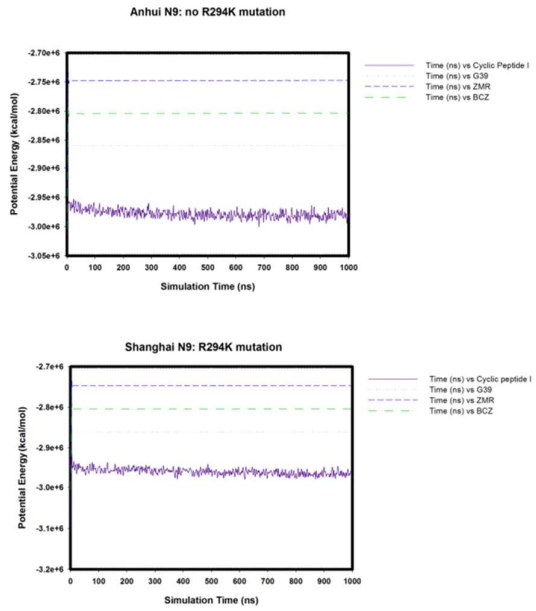

Figure 4. The potential energies of the complex structures (both Anhui and Shanghai N9/cyclic peptide I/G39/ZMR/BCZ) were equilibrated during the 1000 ns simulations.

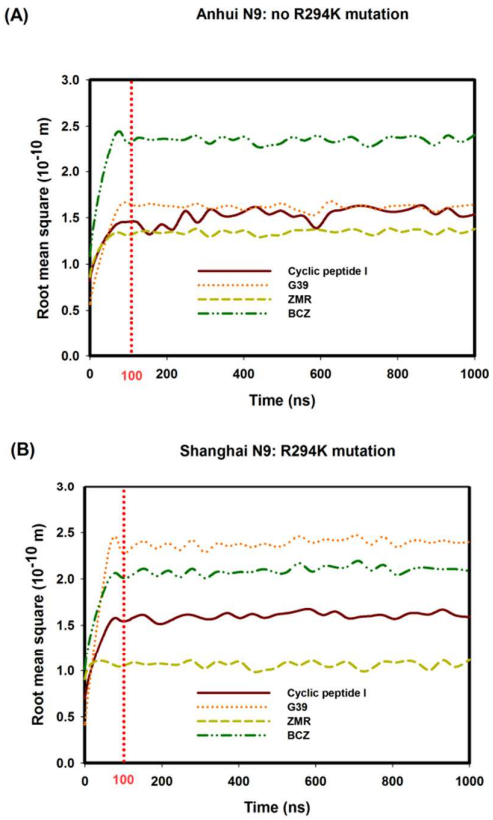

Figure 5. The complex structures (both Anhui and Shanghai N9/cyclic peptide I/G39/ZMR/BCZ) were equilibrated at 100 ns.

3.3 Solvated interaction energies (SIE) method and computational alanine-scanning mutagenesis.

Our binding free energy calculations were performed by the SIE method. The SIE method is a kind of linear interaction energy (LIE) approach.[28-30] The SIE[17] function to estimate protein-ligand free energy is written as:

$$\Delta G_{bind}(\rho, D_{in}, \alpha, \gamma, C) = \alpha \times [E_c(D_{in}) + \Delta G^R_{bind}(\rho, D_{in}) + E_{vdw} + \gamma \Delta MSA(\rho)] + C \quad (1)$$

where E_C and E_{vdw} are the intermolecular Coulomb and van der Waals interaction energies in the bound state, respectively. These values were calculated using the AMBER molecular mechanics force field (FF99SB) with an optimized dielectric constant. ΔG^R_{bind} is the change in the reaction field energy between the bound and free states and is calculated by solving the Poisson equation with the boundary element method program, BRI BEM[31], and using a molecular surface generated with a variable-radius solvent probe.[32] The ΔMSA term is the change in the molecular surface area upon binding. The following parameters are calibrated by fitting to the absolute binding free energies for a set of 99 protein–ligand complexes: AMBER van der Waals radii linear scaling coefficient (ρ), the solute interior dielectric constant (Din), the molecular surface area coefficient (γ), the global proportionality coefficient related to the loss of configurational entropy upon binding (α), and a constant (C).[28] The optimized values of these parameters are α=0.1048, Din=2.25, ρ=1.1, γ=0.0129 kcal/(mol 0.1nm2), and C=−2.89 kcal/mol. The 14 key residues from binding modes analyze were mutated to alanine for computational alanine-scanning mutagenesis calculations. These mutated complex structures then were sampled with 1000 ns MD simulations. Moreover, the final structures from these simulations were used in the SIE calculations. The SIE and computational alanine-scanning mutagenesis calculations were carried out with the sietraj program.[17]

3.4 Neuraminidase enzyme assay protocol.[33]

A standard fluorometric enzyme assay[34] is adapted to measure neuraminidase activity. Producer cell lysates will be transfected with representative neuraminidase constructs are added to neuraminidase fluorogenic substrate 2'-(4-methylumbelliferyl-Nacetylneuraminic acid (4-MUNANA; Sigma) to a final concentration of 100 µmol/L. The reactions will be carried out in 50 µL of 33 mmol/L MES (pH 6.5) containing 4 mmol/L CaCl2 in 96-well black Optiplates (BD Biosciences). A titration of cyclic peptides will be added to the reaction mixtures and then incubated in a 37 °C water bath for 1 hour. The reactions will be terminated by adding 150 µL stop solution containing 0.5 mol/L NaOH (pH 10.7) and 25% ethanol. The fluorescence of released 4-methylumbelliferone will be measured using a spectrophotometer (PerkinElmer). The excitation wavelength will be set at 355 nm, and the emission wavelength will be set at 460 nm. Samples will be done in triplicate and the experiments repeated at least three times. The Shanghai N9 and Anhui N9 are obtained from Sino Biological Inc. The IC_{50} value is calculated by Sigmaplot software.

Conclusions

Cyclic peptides are an unusual class of compounds which are first discovered from microorganisms, due to their broad biological activities, such as antimicrobial, antiviral, immunosuppressive, and antitumor activities. Cyclic peptides are undergoing very active investigation as potential new sources of drugs and antibiotics. They are much more resistant to proteases than a linear peptide chain. This resistance to proteolysis means that they tend to survive the human digestive process. They can also bind proteins in the cell where traditional drugs cannot.[35] The N- to C-terminal cyclic peptides can provide the important principles and strategies that clearly resonate within the world of bioactive peptides and peptide toxins. The ability to transform peptide biologics into stable and orally active constituents represents a major pharmacological achievement. Cyclic peptide drug leads have gained the attention of the pharmaceutical industry. In this article, we used Autodock vina program, Tip3 water solvent model, MD simulations techniques, computational alanine-scanning mutagenesis method and the SIE method to predict the binding affinities in which peramivir (BCZ), oseltamivir (G39), zanamivir (ZMR) and the cyclic peptide I interact with the Shanghai N9 and Anhui N9 influenza A virus neuraminidases. The calculation binding affinities (ΔGbind) of the cyclic peptide I, BCZ, G39 and ZMR inhibitors are very close to the experimental data. From our SIE binding free energies simulations results, the cyclic peptide can can be potential drugs for Shanghai N9 and Anhui N9 influenza A virus disease treatment. For validating the drug-resistance issue, we performed the computational alanine-scanning mutagenesis simulation to study the binding affinities of the cyclic peptide I to Shanghai N9 neuraminidases. The cyclic peptide I can provide the efficient binding affinities to Shanghai N9 neither by the five residues (Arg119, Ile277, Lys294, Arg372 and Tyr406) mutations[1] nor by the 13 residues (Val117, Gln137, Thr149, Hie151, Asp152, Ser154, Ile224, Asn296, Asn347, Asn348, Ile429, Pro433 and Lys434) analyzed by binding mode analysis. But the four residues (Ile150, Arg153, Gln155 and Arg157) can obviously affect the binding interactions among the cyclic peptide. In comparing with the three drugs (BCZ, G39 and ZMR), the IC50 values of the cyclic peptide are greater than the IC50 values of the ZMR and BCZ drugs. The IC50 values of the cyclic peptide are less than the IC50 values of G39 (Shanghai N9). Therefore, our approach theoretically suggests that the cyclic peptide I potential to inhibit the Shanghai N9 and Anhui N9 influenza A virus neuraminidase.

Acknowledgements

The authors would like to thank the Kaohsiung Medical University of the Taiwan and the Ministry of Science and Technology of Taiwan, for supporting this research (Contract No. MOST 103-2113-M-037-007 and KMU-TP103C0).

Notes and references

1. Y. Wu, Y. Bi, C. J. Vavricka, X. Sun, Y. Zhang, F. Gao, M. Zhao, H. Xiao, C. Qin, J. He, W. Liu, J. Yan, J. Qi and G. F. Gao, *Cell Res*, 2013, **23**, 1347-1355.
2. M.-B. Jennifer L, *Antiviral Research*, 2000, **47**, 1-17.
3. S.-Q. Wang, Q.-S. Du and K.-C. Chou, *Biochemical and Biophysical Research Communications*, 2007, **354**, 634-640.
4. Y.-T. Wang, C.-h. Chan, Z.-Y. Su and C.-L. Chen, *Biophysical Chemistry*, 2010, **147**, 74-80.
5. H. Liu, X. Yao, C. Wang and J. Han, *Molecular Pharmaceutics*, 2010, **7**, 894-904.
6. R. E. Amaro, R. V. Swift, L. Votapka, W. W. Li, R. C. Walker and R. M. Bush, *Nat Commun*, 2011, **2**, 388.
7. D. Pan, H. Sun, C. Bai, Y. Shen, N. Jin, H. Liu and X. Yao, *Journal of Molecular Modeling*, 2011, **17**, 2465-2473.
8. S. Chavan, S. Bhayye and M. Sobhia, *Molecular Diversity*, 2011, **15**, 979-987.
9. B. K. Mai and M. S. Li, *Biochemical and Biophysical Research Communications*, 2011, **410**, 688-691.
10. A. Sharma, A. Tendulkar and P. Wangikar, *Medicinal Chemistry Research*, 2011, **20**, 1445-1449.
11. P. M. Colman, *Protein Science*, 1994, **3**, 1687-1696.
12. E. K. Spanakis and D. E. Sellmeyer, *Osteoporos Int*, 2013, DOI: 10.1007/s00198-013-2580-6, 1-4.
13. M. L. Greenberg and N. Cammack, *Journal of Antimicrobial Chemotherapy*, 2004, **54**, 333-340.
14. H.-J. Lee, A. H. Macbeth, J. H. Pagani and W. Scott Young 3rd, *Progress in Neurobiology*, 2009, **88**, 127-151.
15. K. G. Saag, E. Shane, S. Boonen, F. Marín, D. W. Donley, K. A. Taylor, G. P. Dalsky and R. Marcus, *New England Journal of Medicine*, 2007, **357**, 2028-2039.
16. F. Lefèvre, M.-H. Rémy and J.-M. Masson, *Nucleic Acids Research*, 1997, **25**, 447-448.
17. Q. Cui, T. Sulea, J. D. Schrag, C. Munger, M.-N. Hung, M. Naïm, M. Cygler and E. O. Purisima, *Journal of Molecular Biology*, 2008, **379**, 787-802.
18. D. J. Diller, C. Humblet, X. Zhang and L. M. Westerhoff, *Proteins: Structure, Function, and Bioinformatics*, 2010, **78**, 2329-2337.
19. H. Yang, P. J. Carney, J. C. Chang, J. M. Villanueva and J. Stevens, *Journal of Virology*, 2013, **87**, 12433-12446.
20. A. Pedretti, L. Villa and G. Vistoli, *J Comput Aided Mol Des*, 2004, **18**, 167-173.
21. R. Salomon-Ferrer, D. A. Case and R. C. Walker, *Wiley Interdisciplinary Reviews: Computational Molecular Science*, 2013, **3**, 198-210.
22. D. A. Case, V. Babin, J. T. Berryman, R. M. Betz, Q. Cai, D. S. Cerutti, T. E. Cheatham, T. A. D. III, R. E. Duke, H. Gohlke, A. W. Goetz, S. Gusarov, N. Homeyer, P. Janowski, J. Kaus, I. Kolossvary, A. Kovalenko, T. S. Lee, S. LeGrand, T. Luchko, B. M. R. Luo, K. M. Merz, F. Paesani, D. R. Roe, A. Roitberg, C. Sagui, R. Salomon-Ferrer, G. Seabra, C. L. Simmerling, W. Smith, J. Swails, R. C. Walker, J. Wang, R. M. Wolf, X. Wu and P. A. Kollma, *Amber 14*, University of California, San Francisco, 2014.
23. R. Salomon-Ferrer, A. W. Götz, D. Poole, S. Le Grand and R. C. Walker, *Journal of Chemical Theory and Computation*, 2013, **9**, 3878-3888.
24. T. Steinbrecher, J. Latzer and D. A. Case, *Journal of Chemical Theory and Computation*, 2012, **8**, 4405-4412.
25. W. L. Jorgensen, J. Chandrasekhar, J. D. Madura, R. W. Impey and M. L. Klein, *The Journal of Chemical Physics*, 1983, **79**, 926-935.
26. J.-P. Ryckaert, G. Ciccotti and H. J. C. Berendsen, *Journal of Computational Physics*, 1977, **23**, 327-341.
27. T. Darden, D. York and L. Pedersen, *The Journal of Chemical Physics*, 1993, **98**, 10089-10092.
28. A. Perdih, U. Bren and T. Solmajer, *Journal of Molecular Modeling*, 2009, **15**, 983-996.
29. U. Bren, V. Martínek and J. Florián, *The Journal of Physical Chemistry B*, 2006, **110**, 10557-10566.
30. J. Åqvist, C. Medina and J.-E. Samuelsson, *Protein Engineering*, 1994, **7**, 385-391.
31. E. O. Purisima, *Journal of Computational Chemistry*, 1998, **19**, 1494-1504.
32. S. Bhat and E. O. Purisima, *Proteins: Structure, Function, and Bioinformatics*, 2006, **62**, 244-261.
33. M. Potier, L. Mameli, M. Bélisle, L. Dallaire and S. B. Melançon, *Analytical Biochemistry*, 1979, **94**, 287-296.
34. J. Tisoncik-Go, K. Cordero and L. Rong, *Virol. Sin.*, 2013, **28**, 81-91.
35. P. Thapa, M. Espiritu, C. Cabalteja and J.-P. Bingham, *Int J Pept Res Ther*, 2014, **20**, 545-551.